MAGNETIC FLUX TRAPPING IN SUPERCONDUCTING NIOBIUM

C. Benvenuti, S. Calatroni, I.E. Campisi [1], P. Darriulat, C. Durand [2], M.A. Peck, R. Russo and A.-M. Valente

CERN, Geneva, Switzerland.

[1] Scientific Associate on leave from TJNAF, Newport News, Virginia, USA.

[2] Present address: Laboratori Nazionali di Legnaro, Legnaro, PD, Italy.

Presented at the Eighth Workshop on RF Superconductivity

Abano, Italy, 6-10 October 1997

1 Introduction

In a systematic study of the RF response of superconducting niobium cavities operated in their fundamental TM_{010} mode at 1.5 GHz, magnetic flux trapping has been used as a tool to diagnose the presence of pinning centres. In addition to bulk niobium cavities the study covers copper cavities, the inner walls of which are coated with 1.5 μm thick niobium films grown by magnetron sputtering in a noble gas atmosphere. The use of different gases (Xe, Kr, Ar and Ne) or gas mixtures has made it possible to vary the concentration of noble gas atoms in the films. Film contamination is characterised by an electron mean free path ℓ calculated from the results of systematic measurements of the penetration depth at T = 0 K, λ_0, and from RRR measurements made on samples prepared under similar conditions as the cavity films.

2 Experimental Apparatus and Method

A sketch of the apparatus is shown in Fig. 1. The average RF magnetic field (H_{RF}) and surface resistance (R_s) are obtained from spectrum analyser measurements of the incident, reflected and transmitted RF powers. Flux trapping is achieved with the help of a solenoidal coil wound around the cryostat which produces a magnetic field parallel to the cavity axis and uniform over its volume. The coil is surrounded by a μ-metal cylinder which shields the cryostat from the earth field to better than 0.01 G. Care has been taken to prevent the presence of ferromagnetic materials inside the cryostat.

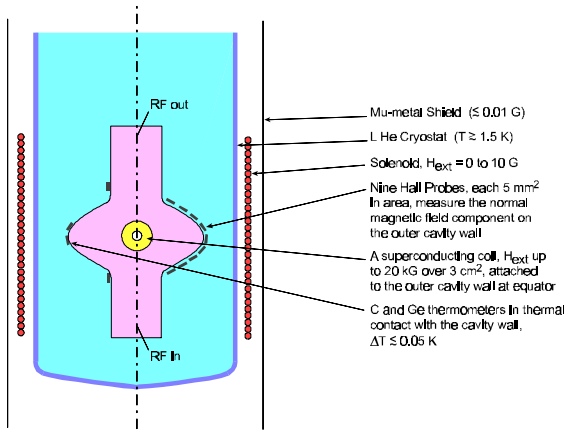

Figure 1

In practice, each measurement implies draining the cryostat and letting the cavity temperature increase above T_c, to typically 20 K, switching the solenoid on at the desired field level H_{ext}, adjustable between 0 and 9 G, and refilling the cryostat with liquid helium (Fig. 2, path 1).

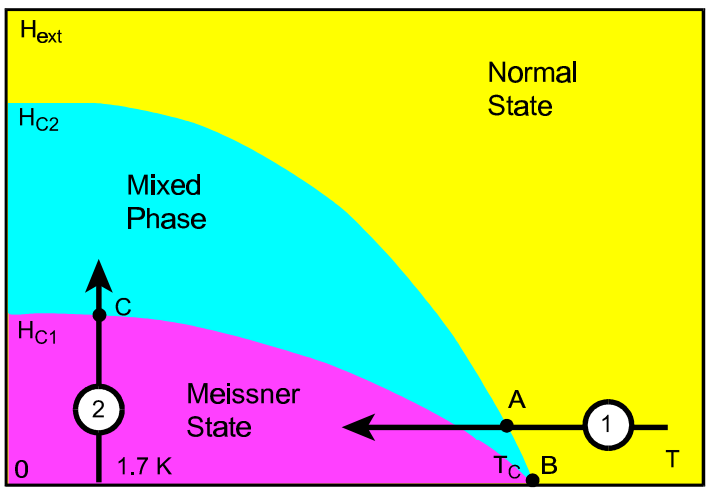

Figure 2

Hall probes distributed along an outer meridian of the resonator are used to measure the normal magnetic field component in the vicinity of the superconductor's surface. As the cavity is cooled down below T_c, it crosses the transition from normal state to mixed phase when the temperature T is such that the upper critical field, $H_{c2}(T) = H_{ext}$. At this time the magnetic flux condenses in a fluxon lattice having a density of 4.8×10^4 mm^{-2} per gauss of H_{ext} , too large to result in a detectable signal on the 5 mm^2 area of each of the Hall probes. When the temperature decreases further and enters the Meissner phase, the Hall probe signal will remain unchanged if the flux is fully trapped, as is usually the case. If, on the contrary, the flux is partly or completely expelled the Hall probe signal will be affected. For each cavity the field discontinuity ΔH detected by each of the Hall probes (with the solenoid on) when crossing the transition upwards is measured in two different configurations, one (ΔH_{on}) when the cavity has been cooled down in $H_{ext} \neq 0$, the other (ΔH_{off}) when the cavity has been cooled down in $H_{ext} = 0$.

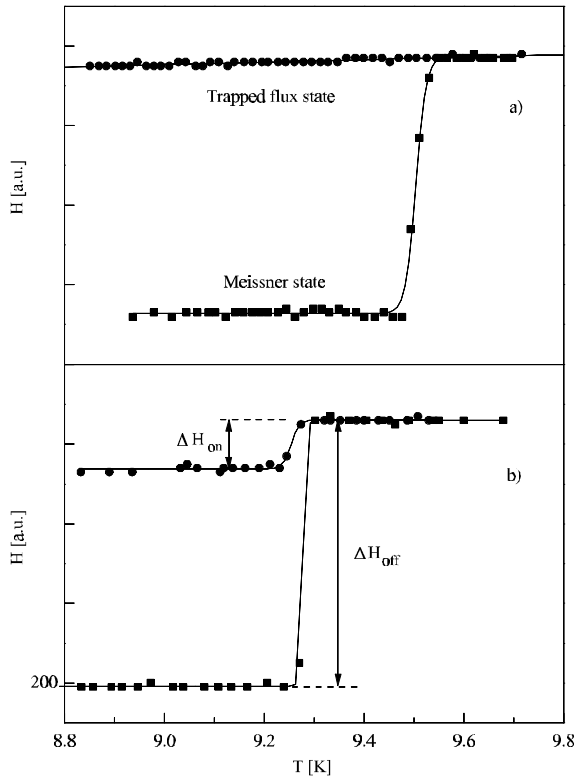

Figure 3

The parameter $\varepsilon = \Delta H_{on}/\Delta H_{off}$ measures the fraction of magnetic flux expelled from the film as it becomes superconducting. When the flux is fully trapped, $\varepsilon = 0$. However, as the Hall probes see only a very small fraction of the cavity area, the extrapolation of this result to the whole surface is only valid if the film is sufficiently homogeneous. In practice, other features give confidence that this is indeed the case. When ε deviates from 0, a situation observed in the case of heat-treated bulk niobium cavities, it is only possible to conclude that a change in fluxon density occurred over the cavity area covered by the Hall probes. However, in this case it is not possible to reliably deduce from the measurement of ε the value of the flux trapping efficiency averaged over the whole cavity area. Examples of such measurements are illustrated in Fig. 3 which displays the magnetic field H measured in one of the Hall probes as a function of temperature. A typical film with full flux trapping is illustrated in Fig. 3a, and a heat-treated bulk niobium cavity with incomplete flux trapping in Fig. 3b. The accuracy of the ε measurement is about 1%.

As a by-product, the jump of ΔH_{off} across T_c provides a measurement of the critical temperature, the width of the transition being only slightly affected by the temperature gradient between the upper and lower parts of the resonator, which is kept below 4 mK/cm over the cavity length.

A small superconducting coil, attached to the external resonator wall at the equator, is used to obtain a relative measurement of the lower critical field at T = 1.7 K, H_{c1}. It can produce a field of up to 20 kG on the film surface. When applied on a cavity cooled down in $H_{ext} = 0$ (the perfect Meissner state) its penetration inside the film signals the transition into the mixed phase, occurring when the field generated by the superconducting coil reaches H_{c1}, and results in a sudden increase of the surface resistance (Fig. 2, path 2).

Figure 4 illustrates a typical measurement. The knee of the curve, obtained from a linear fit to *ln* R_s versus I (the current in the superconducting coil), defines H_{c1}. While the method does not allow an accurate measurement of the absolute value of H_{c1} because of the bad geometry, it provides a good relative measurement when comparing one cavity with another, the geometry being the same in both cases. The dependence of H_{c1} on the mean free path is illustrated in Fig. 5 where H_{c1}^{-2} is displayed as a function of λ_0^2, both quantities being normalised to the values taken in the clean limit, with $\lambda_0^2 = \lambda_{clean}^2 (1+\pi/2(\xi_0/\ell))$ and ξ_0 being the BCS coherence length. The line, drawn as a reference, corresponds to a dependence of the form $H_{c1}^{-2} = \lambda_0^{4/3}$.

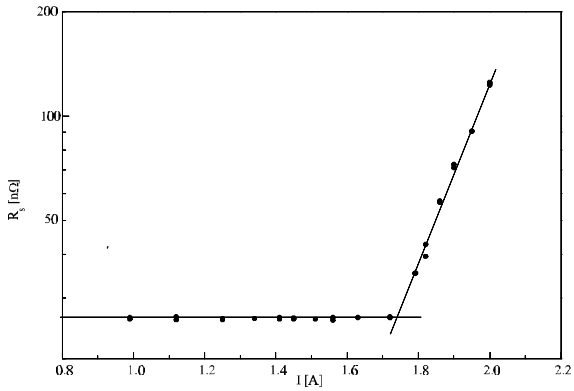

Figure 4

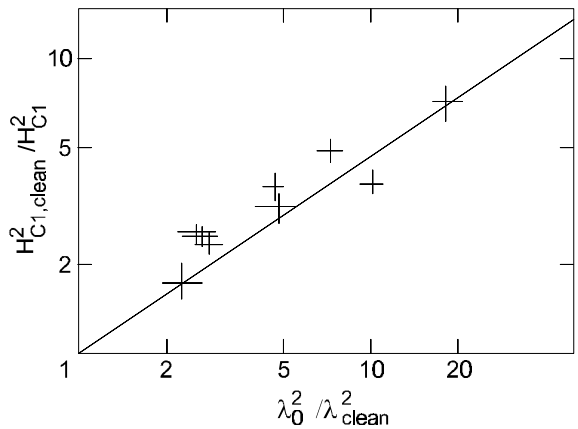

Figure 5

3 Flux trapping efficiency

With the exception of heat-treated bulk niobium, complete trapping was always observed, $\varepsilon < 0.2\%$ to 99% confidence level. Moreover, the trapped state was found to be relatively robust against external perturbations. It was unaffected by switching on and off the solenoid, by the presence of RF power in the cavity, by quenches (corresponding to a brief local increase of the temperature above T_c), and did not significantly evolve over periods of several hours. However, for bulk niobium the measurement method prevents an accurate localisation of the pinning centres. In particular, pinning may occur on the outer surface of the cavity wall and the fluxons may be free to move on the inner surface where the RF field penetrates.

Heat-treated (1000 °C or more) bulk niobium cavities display a lower trapping efficiency, with ε taking different values for different Hall probes, spanning the whole range between 0 and 1 and going hand in hand with a lack of reproducibility of the R_s measurements in successive trapping cycles. Unfortunately, an analysis of the nature of the fluxon movements when crossing the mixed phase would require much more powerful instrumentation than that available in the present experiment. The small area covered by each of the Hall probes, comparable to that of a grain in the heat-treated case, and the bad geometry (the probes being on the outer side of the 3 mm thick niobium wall while the RF field penetrates from the inner side) prevent a reliable interpretation of the data in such cases.

4 Fluxon-induced losses

The fluxon-induced resistance, R_{fl}, is obtained from the difference between data measured with and without trapped flux. It is best measured at $T \leq 1.7$ K where the BCS resistance has become negligible. Its dependence on H_{RF} and H_{ext} is observed to take the form

$$R_{fl}\ (1.7\ K) = (R^0_{fl} + R^1_{fl}\ H_{RF})\ H_{ext}.$$

This is illustrated in Figs. 6 and 7 with data corresponding to films grown in an argon atmosphere (RRR ≅ 15, $\lambda_0^2 \cong 2.5$).

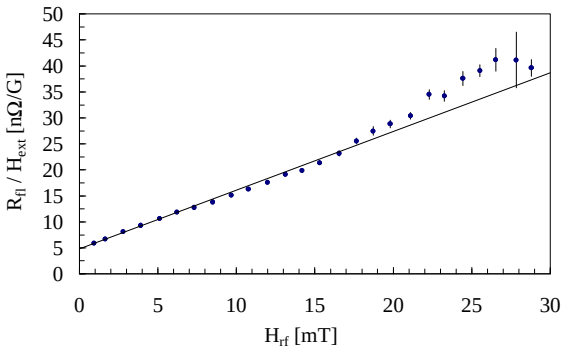

Figure 6

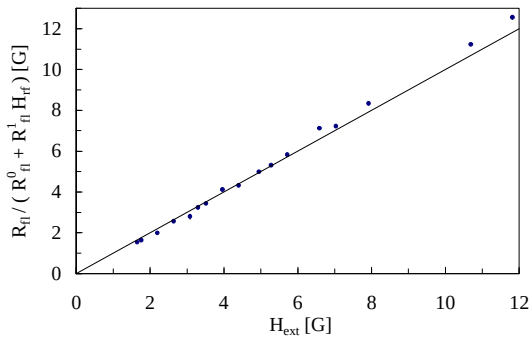

Figure 7

Above a cavity-dependent threshold, possibly correlated with field emission, R_{fl} is often observed to increase faster with H_{RF}. The proportionality to H_{ext} , indicating that the losses induced by different fluxons are uncorrelated, remains valid as long as R_{fl} does not exceed a few hundred nanoOhms, above which a steeper H_{ext} dependence is usually observed.

Films may occasionally display a threshold in H_{ext}, H_{thr}, below which R_{fl} (1.7 K) vanishes. Such films are usually of bad quality, as shown by the large value of their residual resistance. A possible explanation of this particular feature is the presence of a large density of small normal conducting defects (such as pin holes or cracks reaching down to the copper substrate) having dimensions in excess of the coherence length. Flux trapped in such defects does not induce any additional RF loss as the defect was already normal conducting before trapping. The threshold in H_{ext} would then correspond to the saturation of such defects, above which R_{fl} (1.7 K) would increase in proportion to the number of additional trapped fluxons, i.e. to H_{ext}-H_{thr}.

Within the linear range the parameters R^0_{fl} and R^1_{fl} can be used to characterise fluxon-induced losses at low temperature. Figure 8 illustrates their evolution when the mean free path (each data point is labelled with the associated value of λ_0^2) is varied. Minimal losses are observed when the pinning is strongest, corresponding to barely overlapping pinning centres in the thin superficial layer where the RF penetrates. For higher concentrations it takes less energy for a fluxon to jump from one centre to a nearby one under the influence of the RF field, whilst for lower concentrations some fluxons which are not individually

pinned are free to move away from their equilibrium position in the globally pinned lattice. In both cases important flux-flow losses are generated.

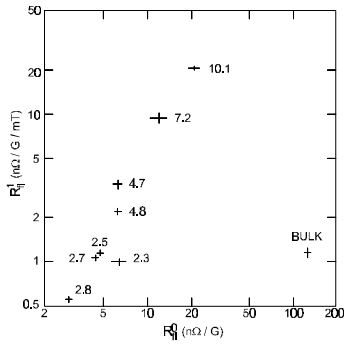

Figure 8

The temperature dependence of R_{fl} is illustrated in Fig. 9 for films grown in an argon atmosphere ($\lambda_0^2 \cong 2.5$). The ratio $R_{fl} = R_{fl}$ (4.2 K) / R_{fl} (1.7 K) is a convenient measure of the amount of temperature dependence. As a function of the mean free path (Fig. 10) it displays a maximum at $\ell \cong \xi_0$, where R_{fl} is minimal.

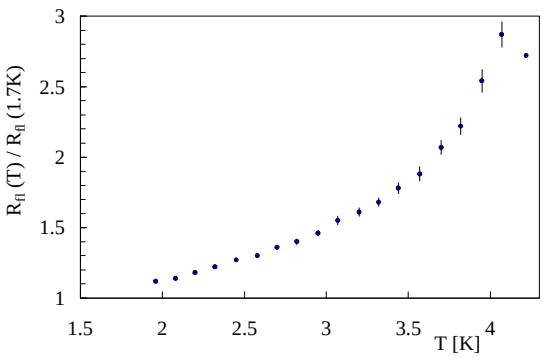

Figure 9

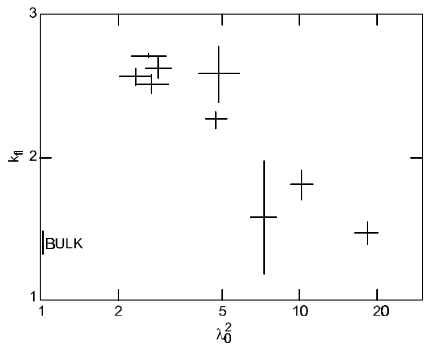

Figure 10

5 Conclusion

The data presented in this short note illustrate how magnetic flux trapping can be used as a tool in the study of the superconducting properties of niobium films. Two parameters, R^0_{fl} and R^1_{fl} , are usually sufficient to describe fluxon-induced RF losses. They span nearly two orders of magnitude when the mean free path is varied from the clean limit to $\ell \cong 0.1\ \xi_0$. They provide information complementary to that obtained from the knowledge of the mean free path, as the pinning and electron scattering mechanisms are of different natures. They can be measured accurately and contribute important information to the understanding of low T_c superconductivity.